AN EXPLORATORY INVESTIGATION OF THE EFFECT OF A PLASTIC COATING ON THE PROFILE DRAG OF A PRACTICAL-METAL-CONSTRUCTION SAILPLANE AIRFOIL

Dan M. Somers
Langley Research Center

SUMMARY

An exploratory investigation was performed in the Langley low-turbulence pressure tunnel to determine the effect of a plastic coating on the profile drag of a practical-metal-construction sailplane airfoil. The model was tested with three surface configurations: (1) filled, painted, and sanded smooth; (2) rough bare metal; and (3) plastic-coated. The investigation was conducted at Reynolds numbers based on airfoil chord of 1.1×10^6, 2.2×10^6, and 3.3×10^6 at a constant Mach number of 0.10.

The results indicate that, at all three Reynolds numbers, the order of the drag values of the three surface configurations, starting with the highest drag, was: filled, painted, and sanded smooth; rough bare metal; and plastic-coated.

INTRODUCTION

Research on advanced technology airfoils has received considerable attention over the past several years at the Langley Research Center. As part of this overall research program, the present investigation was conducted to determine the effect of a plastic coating on the profile drag of a practical-metal-construction sailplane airfoil. Accordingly, a two-dimensional wind-tunnel model was constructed by an American sailplane manufacturer employing the same sheet-metal fabrication techniques used in constructing the corresponding production wing. Three surface configurations were investigated: (1) as received (filled and painted); (2) bare metal; and (3) plastic-coated. The plastic-coating procedure is described in detail in reference 1. The airfoil, which corresponds to the FX 67-K-170/17 airfoil designed by F. X. Wortmann, is representative of state-of-the-art laminar airfoils having variable geometry (in this case, a plain flap). The experimental section characteristics of the FX 67-K-170/17 airfoil are reported in reference 2.

The investigation was performed in the Langley low-turbulence pressure tunnel (ref. 3). The profile-drag coefficients of the three configurations were obtained at Reynolds numbers based on airfoil chord of 1.1×10^6, 2.2×10^6, and 3.3×10^6 at a constant Mach number of 0.10. The geometric angle of attack varied from -5° to 10°. The results have been compared with data from reference 2.

SYMBOLS

c_p	pressure coefficient
c	airfoil chord, cm (in.)
c_d	section profile-drag coefficient, $\int_{wake} c_d' \, d\left(\frac{h}{c}\right)$
c_d'	point drag coefficient (ref. 4)
c_l	section lift coefficient
c_m	section pitching-moment coefficient about quarter-chord point
d	surface-waviness-gage reading, cm (in.)
h	vertical distance in wake profile, cm (in.)
M	free-stream Mach number
R	Reynolds number based on free-stream conditions and airfoil chord
s	arc length from leading edge, cm (in.)
x	airfoil abscissa, cm (in.)
z	airfoil ordinate, cm (in.)
α	angle of attack, deg

MODEL, APPARATUS, AND PROCEDURE

Model

The constant-chord wind-tunnel model was constructed by an American sailplane manufacturer employing the same sheet-metal fabrication techniques used in constructing the corresponding tapered production wing. The structure consisted of a spar and four stringers to which a 0.81 mm (0.032 in.) skin was flush-riveted. In addition, four ribs were flush-riveted to the skin at 30.48-cm (12.00-in.) intervals spanwise. The model had a chord 66.47 cm (26.17 in.) and a span of 91.44 cm (36.00 in.). A plain lower-surface-hinged flap having a chord of 0.17c was fixed at 0^o deflection (fig. 1). The flap gap was sealed with tape along the lower surface. No orifices were installed in the model.

Three surface configurations were investigated (fig. 2). Configuration 1 (as received) (fig. 2(a)) had a factory finish - a painted epoxy primer (filler) -

which had been sanded to insure an aerodynamically smooth surface. Configuration 2 (bare metal) was obtained by chemically removing the paint and primer. (See fig. 2(a).) The surface of configuration 2 (bare metal) was very rough because it had been mechanically roughened at the factory to provide a good bonding surface for the epoxy primer (fig. 3(a)). A plastic film was then bonded to the metal of configuration 2 (bare metal) to obtain configuration 3 (plastic-coated) (figs. 2(b) and 3(b)). It should be noted that the rough surface of configuration 2 (bare metal) can be seen through the plastic film and adhesive of configuration 3 (plastic-coated) (fig. 3(b)). The thickness of the plastic film was approximately 0.1 mm (0.005 in.) whereas the adhesive averaged about 0.25 mm (0.010 in.) in depth. The thickness of the plastic film and the adhesive together was nearly equal to that of the paint and filler as illustrated in figure 2(c). Configuration 1 (as received) and the FX 67-K-170/17 airfoil are compared in figure 2(d). The coordinates of the three configurations together with those of the FX 67-K-170/17 airfoil are listed in table I.

A relative waviness survey was made at the midspan of configuration 3 (plastic-coated). (See fig. 4.) A surface-waviness gage as described in reference 5 was used. The distance between the feet of the gage was approximately 6.4 cm (2.5 in.).

Wind Tunnel

The Langley low-turbulence pressure tunnel (ref. 3) is a closed-throat, single-return tunnel which can be operated at stagnation pressures from 10.13 to 1013 kPa (0.1 to 10 atm) with maximum tunnel-empty test-section Mach numbers of 0.46 and 0.23, respectively. The minimum unit Reynolds number is approximately 0.66×10^6 per meter (0.20×10^6 per foot) at a Mach number of about 0.10, whereas the maximum unit Reynolds number is approximately 49×10^6 per meter (15×10^6 per foot) at a Mach number of 0.23. The test section is 91.44 cm (3.000 ft) wide by 228.6 cm (7.500 ft) high.

Hydraulically actuated circular plates provide positioning and attachment for the two-dimensional model. The plates, 101.6 cm (40.00 in.) in diameter, are flush with the tunnel sidewalls and rotate with the model. The model ends were mounted to rectangular model-attachment plates as shown in figure 5.

Wake-Survey Rake

A fixed, wake-survey rake (fig. 6) was cantilevered from the tunnel sidewall at the model midspan and approximately 0.9 chords downstream from the trailing edge of the model. The wake rake employed 91 total-pressure tubes, 0.152 cm (0.060 in.) in diameter, and 5 static-pressure tubes, 0.318 cm (0.125 in.) in diameter. The total-pressure tubes were flattened to 0.102 cm (0.040 in.) for a length of 0.61 cm (0.24 in.) from the tips of the tubes. Each static-pressure tube had four flush orifices located 90° apart, 8 tube diameters from the tip of the tube in the measurement plane of the total-pressure tubes.

Instrumentation

Measurements of the wake-rake pressures were made by an automatic pressure-scanning system. Basic tunnel pressures as well as the wake-rake pressures were measured with variable-capacitance precision transducers. Geometric angle of attack was measured by a calibrated digital shaft encoder driven by a pinion gear and rack attached to the circular plates. Data were obtained by a high-speed data-acquisition system and were recorded on magnetic tape.

Tests and Methods

The airfoil was tested at Reynolds numbers based on the airfoil chord of 1.1×10^6, 2.2×10^6, and 3.3×10^6 at a Mach number of 0.10 over an angle-of-attack range from -5^o to 10^o. For several test runs, the upper surface of configuration 3 (plastic-coated) was coated with oil to determine the location as well as the nature of the boundary-layer transition from laminar to turbulent.

Section lift coefficients and pitching-moment coefficients about the quarter-chord were determined with the viscous-flow airfoil method of reference 6 because no orifices were installed in the model. Section profile-drag coefficients were computed from the wake-rake total and the wake-rake static pressures by the method of reference 4.

Standard low-speed wind-tunnel boundary corrections (ref. 7), approximately 2 percent of the measured coefficients, have been applied to the drag data.

DISCUSSION

Pressure Distributions

The theoretical chordwise pressure distributions at the approximate limits of the laminar low-drag range are shown in figure 7. At an angle of attack of 0^o ($c_l = 0.5$) which corresponds to the lower limit of the laminar low-drag range, a favorable pressure gradient was predicted on the upper surface to about $x/c = 0.40$ whereas a zero pressure gradient was predicted on the forward portion of the lower surface. As angle of attack was increased, the calculated pressure gradient on the lower surface became more favorable whereas that on the upper surface became less favorable. At an angle of attack of 6^o ($c_l = 1.2$), the upper limit of the low-drag range, a favorable pressure gradient was predicted to about $x/c = 0.60$ on the lower surface whereas a zero pressure gradient was predicted on the forward portion of the upper surface. Between the lower and upper limits of the laminar low-drag range, favorable pressure gradients were predicted on the forward portions of both surfaces.

Section Characteristics

The section characteristics of the three configurations are shown in figure 8 and tabulated in table II. The lift and drag coefficients of the FX 67-K-170/17 airfoil are shown for comparison, having been interpolated from the data of reference 2, which were obtained at Reynolds numbers of 1.0×10^6,

1.5×10^6, 2.0×10^6, and 2.5×10^6. As previously mentioned, both the lift and pitching-moment coefficients of the three configurations were generated by the theoretical method of reference 6, which appears to give excellent agreement with experiment where no trailing-edge separation is present (ref. 8). Accordingly, the c_l - versus - α and the c_l - versus $-c_m$ portions of figure 8 are entirely theoretical whereas the c_l - versus $-c_d$ portion consists of the theoretical lift coefficient plotted against the experimental drag coefficient. No quantitative measure of maximum lift coefficient is possible because of a lack of separation modelling in the theory of reference 6.

The mechanism of boundary-layer transition from laminar to turbulent on this airfoil at these Reynolds numbers is a laminar separation bubble as shown in figure 9 and illustrated in the sketch below.

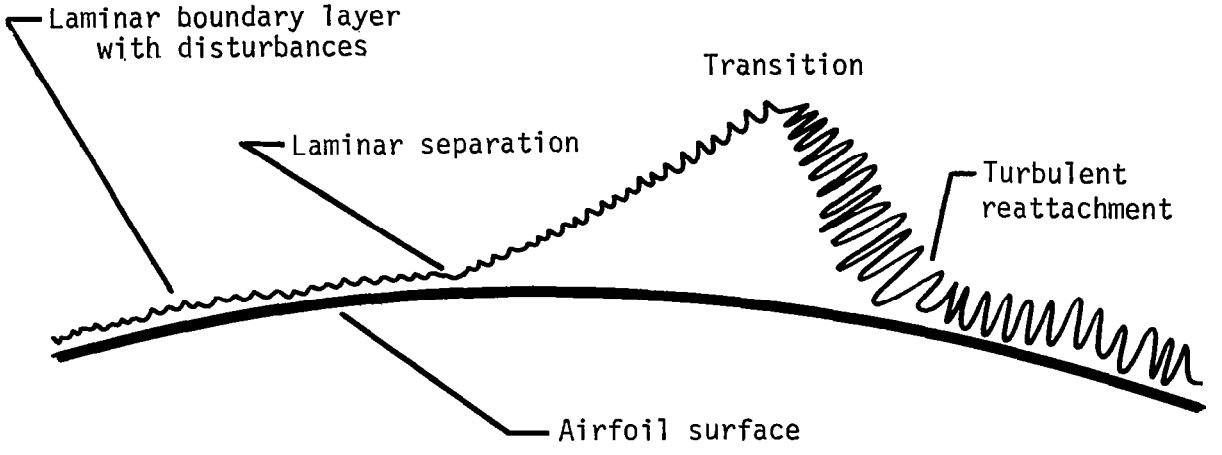

The bubble was caused by a slight adverse pressure gradient immediately downstream of the minimum pressure on the upper surface. (See fig. 7.) This slight adverse gradient was a design feature of the airfoil, as discussed in reference 9.

The section characteristics at a Reynolds number of 1.1×10^6 are shown in figure 8(a). The drag of configuration 1 (as received) was the highest, the drag of configuration 2 (bare metal) lower, and the drag of configuration 3 (plastic-coated) the lowest. The drag coefficients interpolated from the data of reference 2 for the FX 67-K-170/17 airfoil fell between those for configurations 1 (as received) and 2 (bare metal).

One possible explanation for the above order, based upon an understanding of laminar separation bubbles and the data presented in references 9-11, follows. The lower drag coefficients of configurations 2 (bare metal) and 3 (plastic-coated) have been attributed to reductions in the size of the laminar

separation bubble on the upper surface of the airfoil. These reductions were probably caused by two different mechanisms. For configuration 2 (bare metal), introduction of additional disturbances into the laminar boundary layer by the roughness of the surface (fig. 3(a)) apparently did not cause premature transition because they were too small. Once the laminar boundary layer had separated, however, the disturbances would grow rapidly, resulting in transition and, finally, turbulent reattachment. These additional disturbances, therefore, probably reduced the distance between laminar separation and transition (i.e., a shorter bubble). For configuration 3 (plastic-coated), introduction of disturbances into the laminar boundary layer by the waviness of the surface apparently affected the length of the laminar separation bubble as did the disturbances caused by the roughness of configuration 2 (bare metal) with an even shorter bubble for configuration 3 (plastic-coated). The waviness of the configuration 3 (plastic-coated) surface (fig. 4) was probably caused by hand application of the plastic film on very thin sheet metal.

The section characteristics at Reynolds numbers of 2.2×10^6 and 3.3×10^6 are shown in figures 8(b) and 8(c), respectively. The drag of configuration 1 (as received) was again the highest, the drag of configuration 2 (bare metal) was lower, and the drag of configuration 3 (plastic-coated) was again the lowest. The drag coefficients interpolated from the data of reference 2 for the FX 67-K-170/17 airfoil were higher than those for configuration 1 (as received) at a Reynolds number of 2.2×10^6. The explanation for these results is probably the same as that for a Reynolds number of 1.1×10^6.

Results similar to those described above have been reported by other investigators. A substantial drag reduction was obtained by using a trip wire to eliminate the laminar separation bubble on the upper surface of an airfoil (ref. 9). Reductions in the sizes of the laminar separation bubbles on two different airfoils through the introduction of disturbances by roughness and trip wires were reported in references 10 and 11, respectively.

SUMMARY OF RESULTS

An exploratory investigation was performed in the Langley low-turbulence pressure tunnel to determine the effect of a plastic coating on the profile drag of a practical-metal-construction sailplane airfoil. The model was tested with three surface configurations: (1) filled, painted, and sanded smooth; (2) rough bare metal; and (3) plastic-coated. The resulting data have been compared with data for the design airfoil (Wortmann FX 67-K-170/17) from another low-turbulence wind tunnel. The investigation was conducted at Reynolds numbers based on airfoil chord of 1.1×10^6, 2.2×10^6 and 3.3×10^6 at a constant Mach number of 0.10.

At all three Reynolds numbers, the drag of the filled, painted, and sanded smooth configuration was the highest, followed by the drag of the rough bare metal configuration, and finally the drag of the plastic-coated configuration.

REFERENCES

1. Beasley, William D. and McGhee, Robert J.: An Exploratory Investigation of the Effects of a Thin Plastic Film Cover on the Profile Drag of an Aircraft Wing Panel. NASA TM 74073, 1977.

2. Althaus, D.: MeBergebnisse aus dem Laminarwindkanal des Instituts für Aerodynamik und Gasdynamik der Universität Stuttgart. Stuttgarter Profilkatalog I, Institut für Aerodynamik und Gasdynamik der Universität Stuttgart, 1972.

3. Von Doenhoff, Albert E. and Abbott, Frank T., Jr.: The Langley Two-Dimensional Low-Turbulence Pressure Tunnel. NACA TN 1283, 1947.

4. Pankhurst, R. C. and Holder, D. W.: Wind-Tunnel Technique. Sir Isaac Pitman & Sons, Ltd. (London), 1952.

5. Braslow, Albert L.; Burrows, Dale L.; Tetervin, Neal; and Visconti, Fioravante: Experimental and Theoretical Studies of Area Suction for the Control of the Laminar Boundary Layer on an NACA 64A010 Airfoil. NACA Rep. 1025, 1951.

6. Smetana, Frederick O.; Summey, Delbert C.; Smith, Neill S.; and Carden, Ronald K.: Light Aircraft Lift, Drag, and Moment Prediction - A Review and Analysis. NASA CR-2523, 1975.

7. Allen, H. Julian; and Vincenti, Walter G.: Wall Interference in a Two-Dimensional-Flow Wind Tunnel, With Consideration of the Effect of Compressibility. NACA Rep. 782, 1944. (Supersedes NACA WR A-63.)

8. Somers, Dan M.: Experimental and Theoretical Low-Speed Aerodynamic Characteristics of a Wortmann Airfoil as Manufactured on a Fiberglass Sailplane. NASA TN D-8324, 1977.

9. Wortmann, F. X.: Experimental Investigations on New Laminar Profiles for Gliders and Helicopters. TIL/T.4906, British Minist. Aviat., March 1960.

10. Hurley, D. G.: The Downstream Effect of a Local Thickening of the Laminar Boundary Layer. Aeronautical Research Laboratories (Australia) Aerodynamics Note 146, July 1955.

11. Harris, K. D.: The Effect of Transition Wires on the Pressure Distributions over a N.A.C.A. 63A215 Aerofoil Section. The College of Aeronautics (Cranfield), Technical Note 41, 1956.

TABLE I.- AIRFOIL COORDINATES

(a) Configuration 1 (as received)

[c = 66.4827 cm (26.1743 in.)]

Upper surface		Lower surface	
x/c	z/c	x/c	z/c
0.000000	0.000000	0.000000	0.000000
.000004	-.000042	-.000008	-.000038
.000497	.004443	.000500	-.002048
.000993	.005651	.001001	-.003026
.001490	.006827	.001490	-.003805
.001987	.007721	.002017	-.004489
.002980	.009452	.002988	-.005391
.003973	.011133	.003992	-.006185
.004982	.012722	.004986	-.006839
.006980	.015611	.006980	-.007943
.009968	.019389	.009968	-.009360
.014957	.024635	.014950	-.011274
.019939	.029055	.019932	-.013127
.029907	.036658	.029907	-.015611
.039879	.043390	.039879	-.017712
.049843	.049549	.049850	-.019515
.059814	.055214	.059814	-.021063
.069782	.060498	.069786	-.022427
.079754	.065381	.079754	-.023680
.089725	.070080	.089725	-.024677
.099693	.074363	.099689	-.025735
.119633	.082123	.119636	-.027550
.149540	.092274	.149540	-.029773
.199386	.106295	.199386	-.032016
.249225	.116867	.249237	-.033212
.299087	.124687	.299080	-.034221
.348922	.130342	.348922	-.035031
.398773	.133142	.398769	-.035500
.448627	.132928	.448623	-.034924
.498466	.129925	.498470	-.033602
.548301	.124095	.548313	-.031749
.598163	.114696	.598159	-.028734
.648017	.101921	.648006	-.024612
.697845	.086738	.697852	-.020153
.747699	.070241	.747703	-.015389
.797538	.053824	.797546	-.010468
.847392	.037896	.847392	-.006823
.897247	.026320	.897231	-.001941
.947089	.012975	.947085	.001242
.967025	.008638	.967029	.000455
.976997	.006629	.976993	-.000317
.986964	.004569	.986964	-.001035
1.000000	.001486	.999828	-.001284

TABLE I.- AIRFOIL COORDINATES - Continued

(b) Configuration 2 (bare metal)

[c = 66.4670 cm (26.1681 in.)]

Upper surface		Lower surface	
x/c	z/c	x/c	z/c
0.000000	0.000000	0.000000	0.000000
.000050	..000000	.000046	.000000
.000520	.003604	.000501	-.002109
.000994	.004632	.001376	-.004330
.001490	.005568	.001494	-.004548
.001987	.006370	.001987	-.005381
.002992	.008117	.002992	-.006496
.003986	.009749	.003990	-.007184
.004987	.011342	.004979	-.007819
.006955	.014227	.006993	-.008931
.009966	.018075	.009966	-.010433
.014957	.023238	.014949	-.012508
.019944	.027568	.019936	-.014132
.029914	.035069	.029918	-.016730
.039884	.041807	.039892	-.018832
.049855	.047856	.049858	-.020552
.059832	.053542	.059836	-.022061
.069799	.058827	.069810	-.023364
.079777	.063746	.079784	-.024564
.089747	.068255	.089747	-.025627
.099721	.072543	.099724	-.026723
.119661	.080262	.119665	-.028489
.149579	.090385	.149583	-.030694
.199434	.104536	.170547	-.042151
.249292	.115190	.249288	-.033166
.299162	.123020	.299154	-.034683
.349005	.128653	.348997	-.035532
.398871	.131511	.398886	-.036090
.448726	.131064	.448745	-.035731
.498592	.128087	.498603	-.034404
.548443	.122191	.548443	-.032326
.598297	.112702	.598312	-.029295
.648171	.099874	.648167	-.024966
.698014	.084599	.698010	-.020380
.747876	.067773	.747865	-.015947
.797735	.051677	.797735	-.011487
.847589	.036457	.847593	-.007341
.897455	.024645	.897436	-.003424
.947314	.012198	.947314	-.000910
.967254	.007417	.967262	-.000657
.977243	.005583	.977232	-.000703
.987290	.002939	.987271	-.000734
.999889	.000046	1.000000	-.000378

TABLE I.- AIRFOIL COORDINATES - Continued

(c) Configuration 3 (plastic-coated)

[c = 66.4860 cm (26.1756 in.)]

Upper surface		Lower surface	
x/c	z/c	x/c	z/c
0.000000	0.000000	0.000000	0.000000
-.000023	.000061	.000997	-.002124
.000508	.005108	.001494	-.003266
.001016	.006449	.002006	-.003973
.001494	.007664	.002995	-.005058
.001998	.008607	.003985	-.005891
.002991	.010017	.004989	-.006582
.003988	.011522	.006984	-.007683
.004978	.012978	.009963	-.009077
.006972	.015935	.014964	-.011136
.009960	.019904	.019935	-.012817
.014960	.025111	.029898	-.015369
.019938	.029356	.039873	-.017470
.029898	.036943	.049844	-.019213
.039858	.043674	.059815	-.020710
.049844	.049772	.069786	-.022085
.059811	.055414	.079746	-.023235
.069783	.060671	.089713	-.024339
.079746	.065634	.099696	-.025417
.089725	.070222	.119634	-.026991
.099688	.074432	.149544	-.029302
.119634	.082168	.199369	-.031399
.149540	.092517	.249228	-.032599
.199377	.106561	.299069	-.033432
.249221	.117101	.348917	-.034211
.299069	.125105	.398742	-.034830
.348905	.130603	.448593	-.034547
.398749	.133323	.498441	-.033069
.448593	.132983	.548282	-.031124
.498445	.130102	.598122	-.028175
.548285	.124181	.647985	-.024259
.598130	.114786	.697806	-.019388
.647981	.102202	.747666	-.014789
.697818	.087146	.797510	-.010208
.747654	.070237	.847350	-.006284
.797518	.053909	.897179	-.002124
.847346	.038440	.947042	.000004
.897194	.027927	.967015	.000531
.947046	.014960	.976944	.000604
.966985	.010823	.986923	.000714
.976956	.008496	1.000000	.001108
.988837	.005998		
.999924	.003687		

TABLE I.- AIRFOIL COORDINATES - Concluded

(d) FX 67-K-170/17 airfoil

Upper surface		Lower surface	
x/c	z/c	x/c	z/c
0.00000	0.00000	0.00000	0.00000
.00107	.00653	.00107	-.00217
.00428	.01292	.00428	-.00514
.00961	.02012	.00961	-.00815
.01704	.02765	.01704	-.01057
.02653	.03487	.02653	-.01321
.03806	.04309	.03806	-.01580
.05156	.05158	.05156	-.01827
.06699	.06011	.06699	-.02062
.08427	.06856	.08427	-.02282
.10332	.07685	.10332	-.02490
.12408	.08490	.12408	-.02682
.14645	.09263	.14645	-.02856
.17033	.09994	.17033	-.03011
.19562	.10677	.19562	-.03146
.22221	.11305	.22221	-.03261
.25000	.11870	.25000	-.03354
.27866	.12365	.27866	-.03425
.30866	.12783	.30866	-.03474
.33928	.13119	.33928	-.03499
.37059	.13370	.37059	-.03501
.40245	.13526	.40245	-.03480
.43474	.13571	.43474	-.03435
.46730	.13490	.46730	-.03365
.50000	.13274	.50000	-.03272
.53270	.12919	.53270	-.03155
.56526	.12429	.56526	-.03012
.59755	.11808	.59755	-.02844
.62941	.11063	.62941	-.02654
.66072	.10208	.66072	-.02437
.69134	.09263	.69134	-.02187
.72114	.08259	.72114	-.01896
.75000	.07233	.75000	-.01572
.77779	.06229	.77779	-.01236
.80438	.05287	.80438	-.00913
.82967	.04437	.82967	-.00625
.85355	.03689	.85355	-.00386
.87592	.03040	.87592	-.00197
.91573	.01991	.91573	-.00037
.94844	.01201	.94844	-.00124
.97347	.00631	.97347	-.00105
.99039	.00243	.99039	-.00044
.99893	.00027	.99893	-.00005
1.00000	0.00000	1.00000	0.00000

TABLE II.- SECTION CHARACTERISTICS

(a) $R \approx 1.1 \times 10^6$, $M = 0.10$

c_l	α, deg	c_d	c_m
Configuration 1 (as received)			
-.020	-5.05	.0130	-.0978
.080	-4.13	.0117	-.0986
.199	-3.07	.0109	-.1043
.294	-2.09	.0101	-.1055
.412	-1.05	.0082	-.1087
.530	-.00	.0086	-.1120
.650	1.07	.0086	-.1152
.755	2.02	.0084	-.1178
.867	3.07	.0084	-.1203
.974	4.12	.0080	-.1224
1.072	5.12	.0082	-.1231
1.190	6.18	.0079	-.1270
1.297	7.13	.0075	-.1310
1.410	8.22	.0078	-.1345
1.512	9.27	.0079	-.1366
1.602	10.24	.0090	-.1390
Configuration 2 (bare metal)			
-.060	-5.12	.0126	-.0906
.035	-4.21	.0117	-.0925
.162	-3.04	.0110	-.0950
.260	-2.11	.0101	-.0965
.363	-1.03	.0073	-.0980
.477	.01	.0069	-.1003
.585	.99	.0072	-.1023
.694	1.99	.0074	-.1045
.803	3.03	.0072	-.1067
.915	4.07	.0076	-.1091
1.026	5.13	.0078	-.1122
1.139	6.14	.0082	-.1157
1.255	7.21	.0077	-.1195
1.357	8.19	.0071	-.1224
1.441	9.19	.0076	-.1232
1.543	10.27		-.1247
Configuration 3 (plastic-coated)			
-.090	-5.10	.0123	-.0848
.022	-4.08	.0110	-.0870
.130	-3.10	.0100	-.0894
.230	-2.05	.0090	-.0913
.345	-1.04	.0072	-.0940
.465	.02	.0066	-.0967
.575	1.03	.0068	-.0992
.685	2.04	.0070	-.1015
.795	3.06	.0068	-.1035
.898	4.05	.0068	-.1052
1.010	5.10	.0071	-.1082
1.120	6.11	.0072	-.1118
1.233	7.12	.0069	-.1153
1.340	8.16	.0069	-.1172
1.425	9.16	.0074	-.1187
1.522	10.17	.0115	-.1210

TABLE II.- Continued

(b) $R \approx 2.2 \times 10^6$, $M = 0.10$

c_l	α, deg	c_d	c_m
Configuration 1 (as received)			
-.020	-5.05	.0096	-.0979
.090	-4.05	.0095	-.1006
.204	-3.02	.0090	-.1037
.307	-2.06	.0083	-.1062
.420	-1.04	.0059	-.1093
.538	.01	.0057	-.1127
.655	1.03	.0057	-.1159
.770	2.06	.0056	-.1193
.885	3.09	.0060	-.1223
.995	4.09	.0062	-.1250
1.105	5.13	.0064	-.1275
1.220	6.19	.0064	-.1292
1.305	7.14	.0065	-.1303
1.400	8.20	.0067	-.1345
1.505	9.32	.0093	-.1365
1.600	10.29	.0224	-.1392
Configuration 2 (bare metal)			
-.067	-5.14	.0103	-.0905
.037	-4.20	.0096	-.0927
.170	-3.00	.0094	-.0955
.281	-1.96	.0085	-.0977
.378	-1.01	.0063	-.0996
.487	-.02	.0056	-.1020
.613	1.04	.0056	-.1054
.727	2.08	.0054	-.1078
.839	3.05	.0056	-.1096
.936	4.07	.0060	-.1113
1.039	5.10	.0063	-.1132
1.154	6.15	.0066	-.1164
1.260	7.17	.0062	-.1190
1.352	8.26	.0084	-.1220
1.442	9.30		-.1232
1.527	10.18		-.1250
Configuration 3 (plastic-coated)			
-.089	-5.08	.0098	-.0848
.025	-4.06	.0092	-.0874
.140	-3.03	.0088	-.0899
.246	-2.03	.0082	-.0922
.360	-1.00	.0061	-.0950
.473	.01	.0053	-.0977
.590	1.05	.0053	-.1008
.708	2.08	.0053	-.1038
.817	3.06	.0055	-.1065
.930	4.10	.0057	-.1087
1.035	5.15	.0057	-.1100
1.143	6.18	.0058	-.1120
1.247	7.15	.0058	-.1152
1.333	8.17	.0061	-.1175
1.417	9.16	.0107	-.1193
1.518	10.18		-.1215

TABLE II.- Concluded

(c) $R \approx 3.3 \times 10^6$, $M = 0.10$

c_l	α, deg	c_d	c_m
Configuration 1 (as received)			
-.027	-5.09	.0084	-.0977
.090	-4.03	.0081	-.1007
.542	-.02	.0050	-.1130
.657	1.00	.0050	-.1164
.775	2.02	.0050	-.1197
.893	3.08	.0053	-.1230
1.005	4.08	.0055	-.1260
1.111	5.09	.0060	-.1288
1.207	6.11	.0063	-.1307
1.293	7.13	.0060	-.1295
1.389	8.14	.0076	-.1330
1.487	9.15	.0093	-.1365
1.595	10.25		-.1395
Configuration 2 (bare metal)			
-.067	-5.14	.0093	-.0906
.053	-4.06	.0085	-.0932
.158	-3.12	.0084	-.0955
.275	-2.09	.0078	-.0980
.394	-.99	.0066	-.1008
.498	.01	.0050	-.1030
.610	1.00	.0049	-.1058
.737	2.07	.0047	-.1094
.849	3.09	.0049	-.1116
.950	4.09	.0052	-.1127
1.060	5.17	.0057	-.1150
1.160	6.12	.0058	-.1170
1.255	7.19	.0056	-.1185
1.340	8.18	.0099	-.1210
1.437	9.23		-.1237
1.533	10.23		-.1255
Configuration 3 (plastic-coated)			
-.099	-5.14	.0089	-.0847
.025	-4.06	.0081	-.0875
.138	-3.05	.0079	-.0910
.248	-2.05	.0075	-.0926
.367	-1.00	.0061	-.0955
.477	.02	.0046	-.0983
.596	1.04	.0048	-.1015
.710	2.03	.0047	-.1045
.827	3.06	.0047	-.1074
.942	4.10	.0050	-.1102
1.052	5.10	.0053	-.1130
1.150	6.14	.0058	-.1130
1.245	7.16	.0057	-.1149
1.328	8.18	.0073	-.1170
1.420	9.19	.0308	-.1195
1.523	10.19	.0799	-.1219

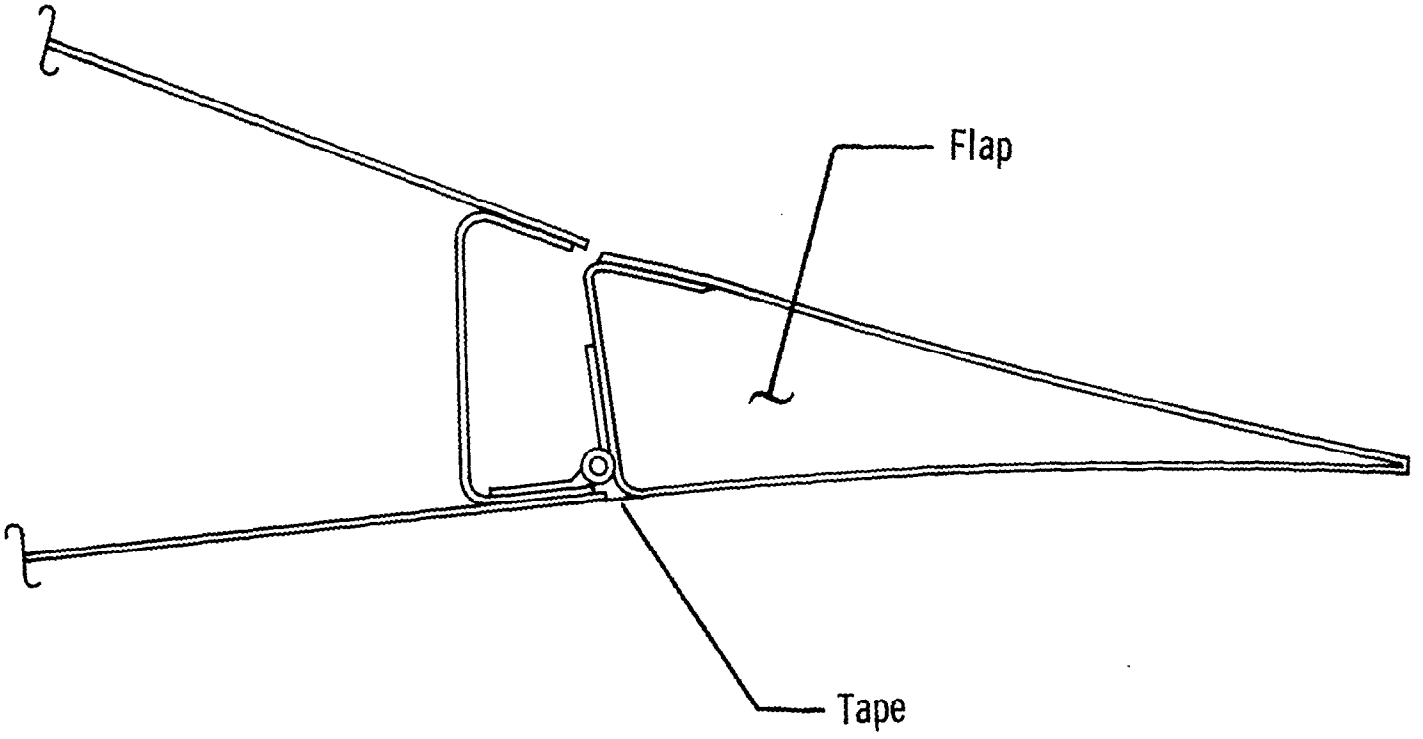

Figure 1.- Flap geometry.

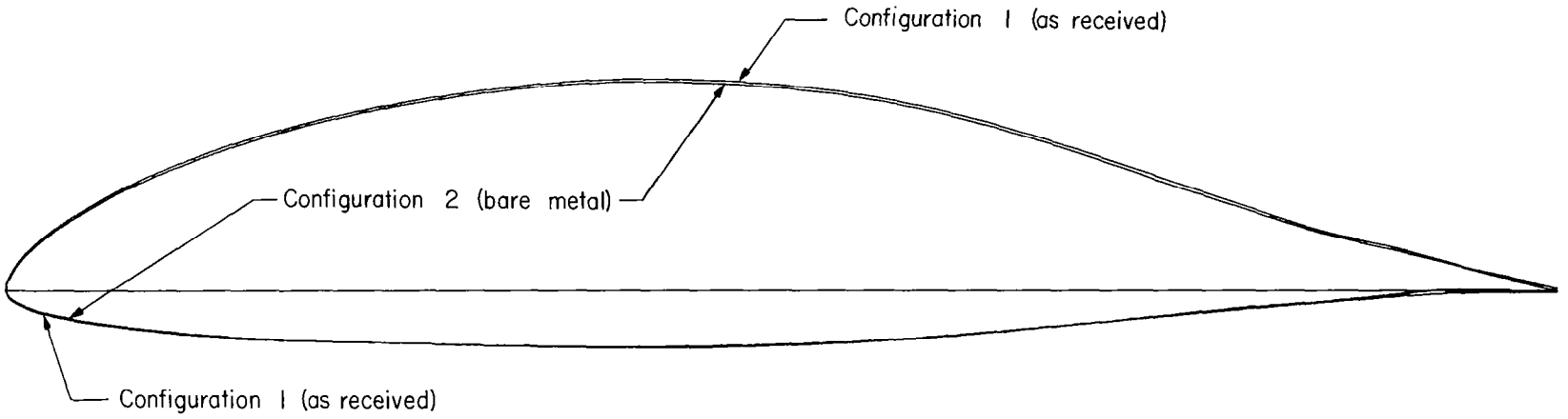

(a) Configurations 1 (as received) and 2 (bare metal).

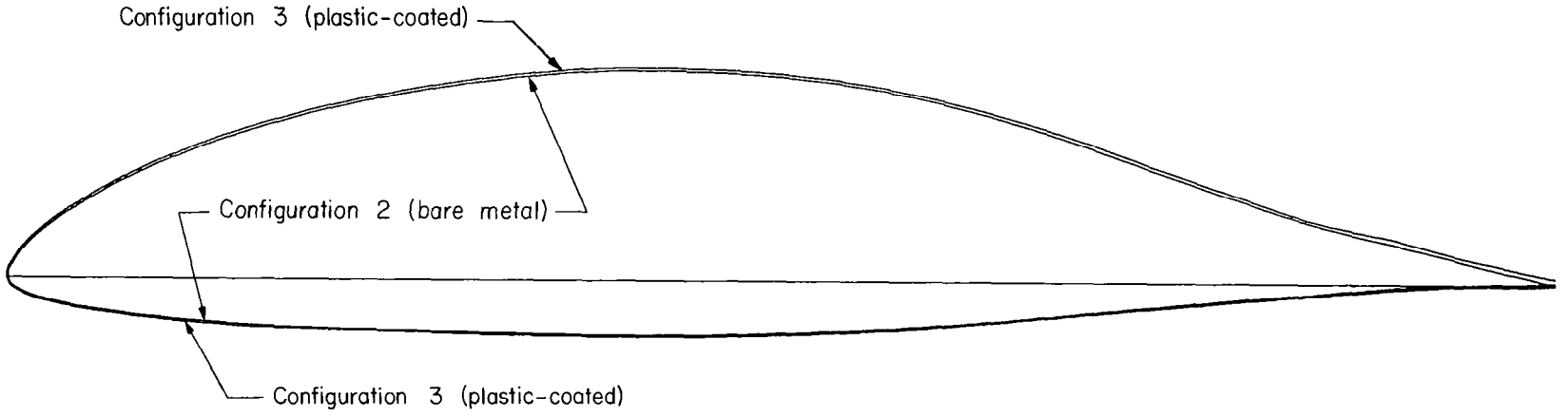

(b) Configurations 2 (bare metal) and 3 (plastic-coated).

Figure 2.- Comparisons of configurations 1 (as received), 2 (bare metal), 3 (plastic-coated), and FX 67-K-170/17 ordinates.

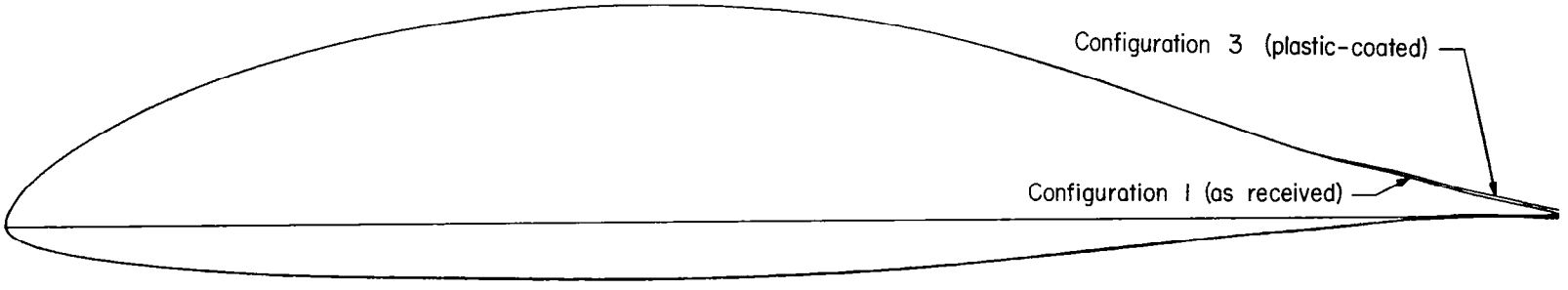

(c) Configurations 1 (as received) and 3 (plastic-coated).

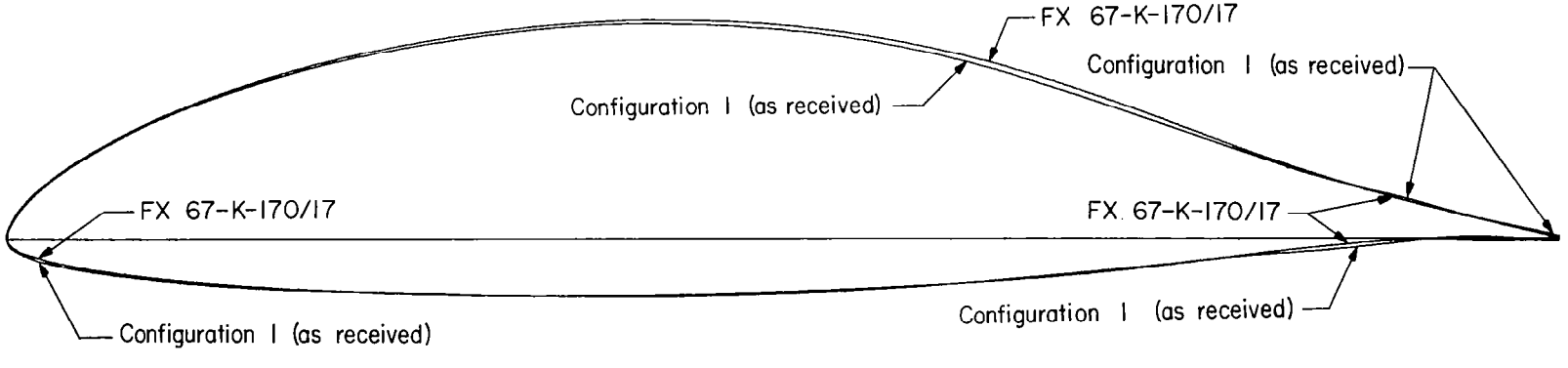

(d) Configuration 1 (as received) and FX 67-K-170/17.

Figure 2.- Concluded.

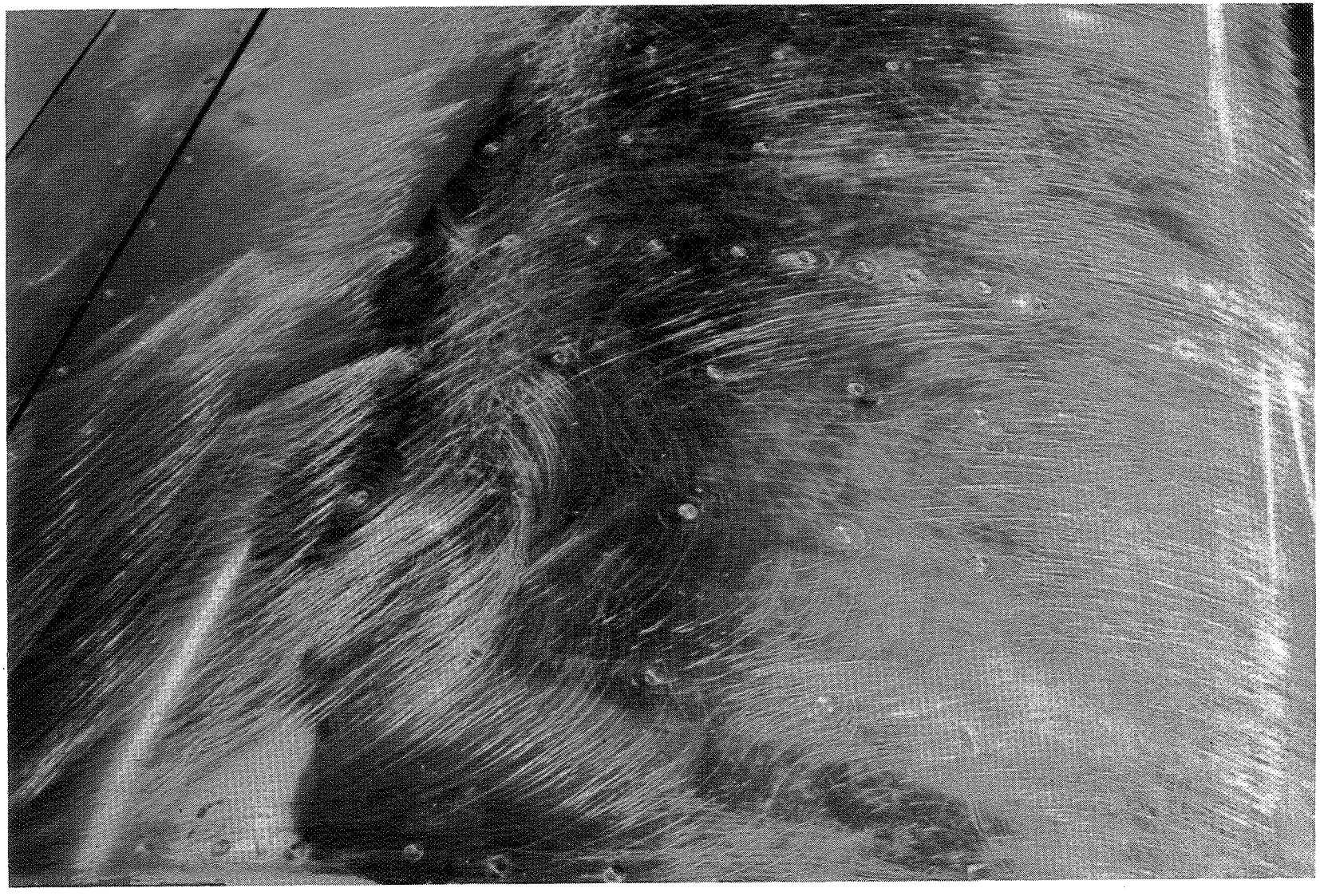

(a) Configuration 2 (bare metal).

Figure 3.- Surfaces of configurations 2 (bare metal) and 3 (plastic-coated).

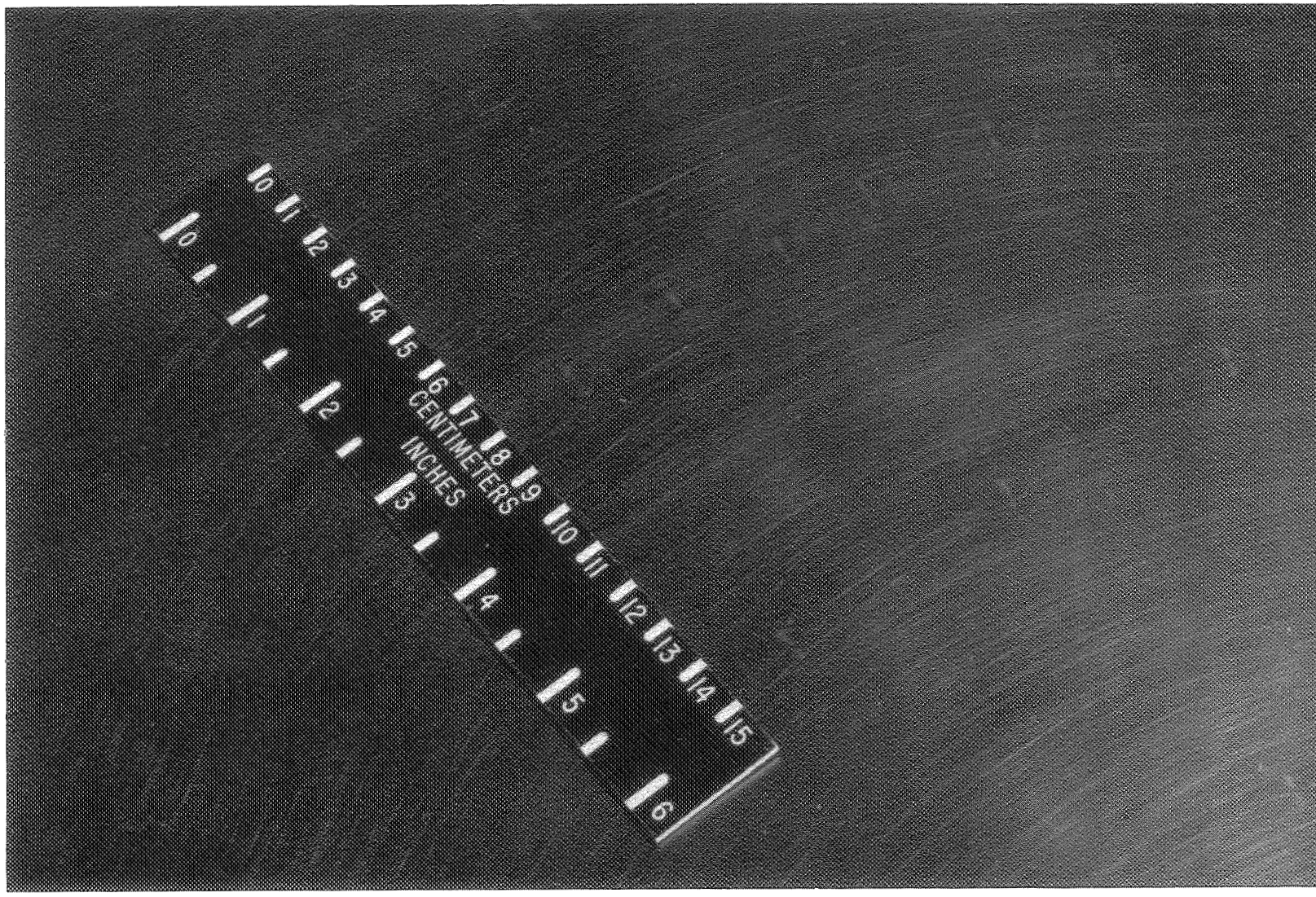

(b) Configuration 3 (plastic-coated).

Figure 3.- Concluded.

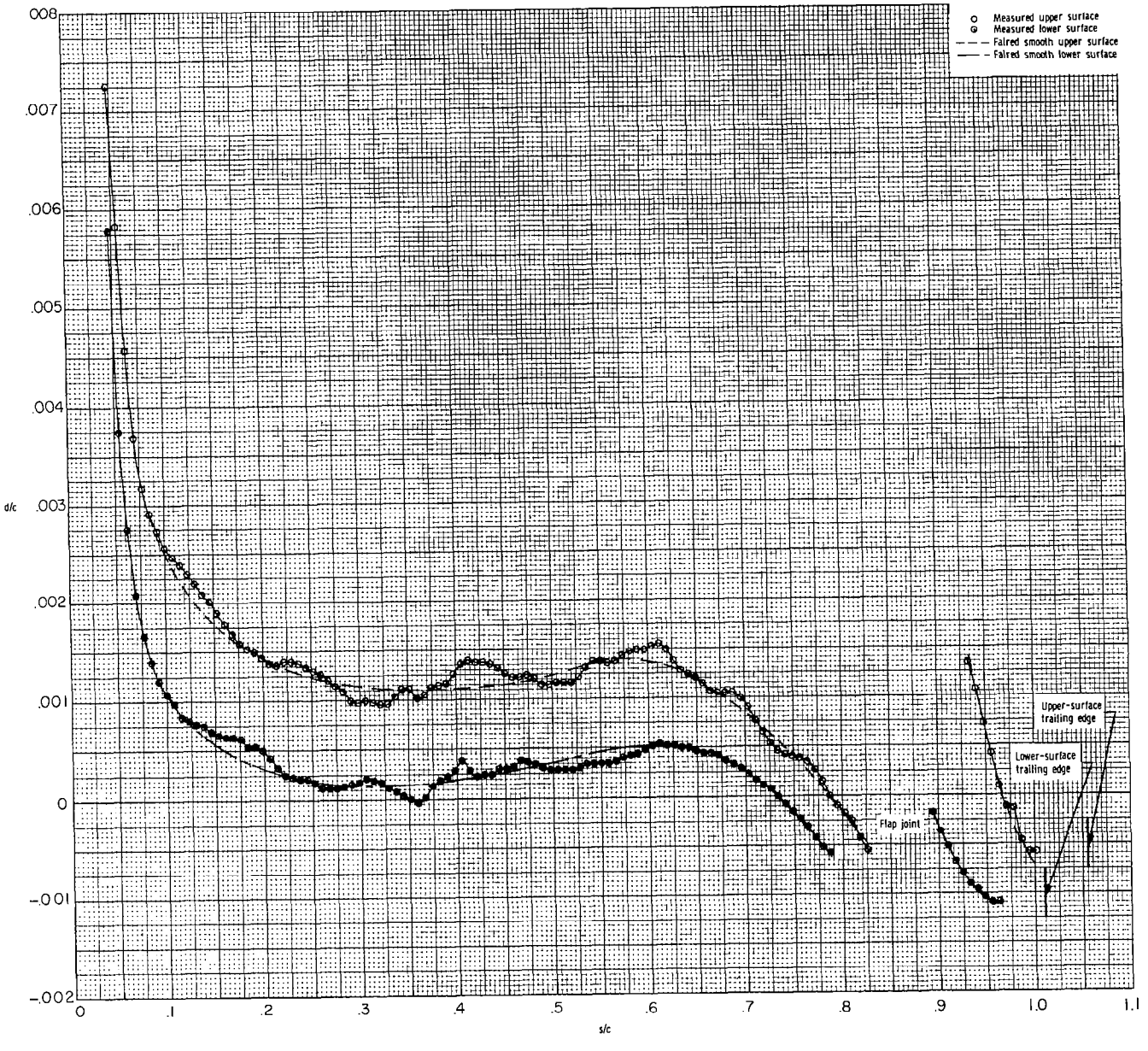

Figure 4.- Surface waviness of configuration 3 (plastic-coated).

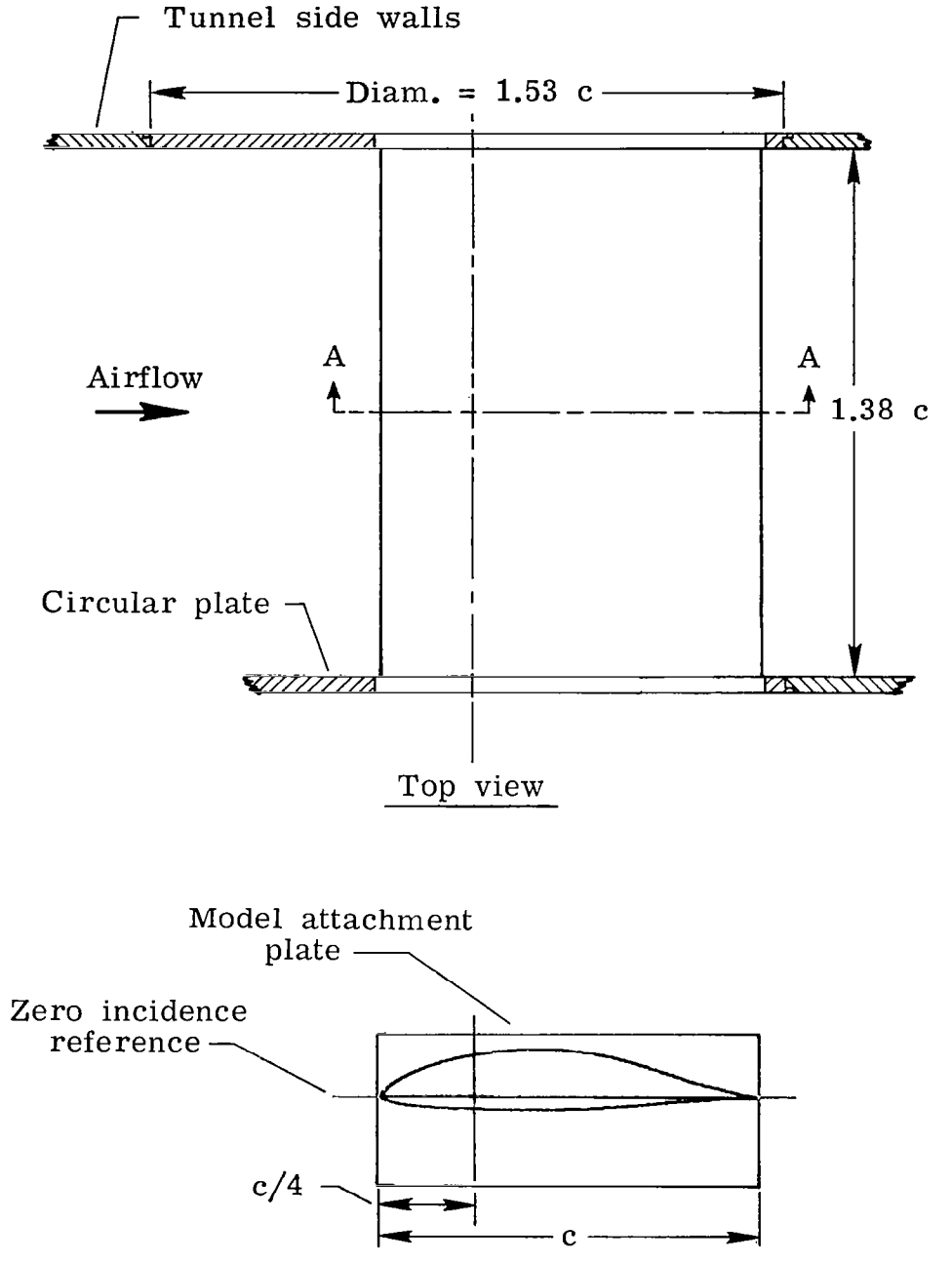

Figure 5.- Airfoil model mounted in wind tunnel. All dimensions are in terms of model chord, c = 66.47 cm (26.17 in.).

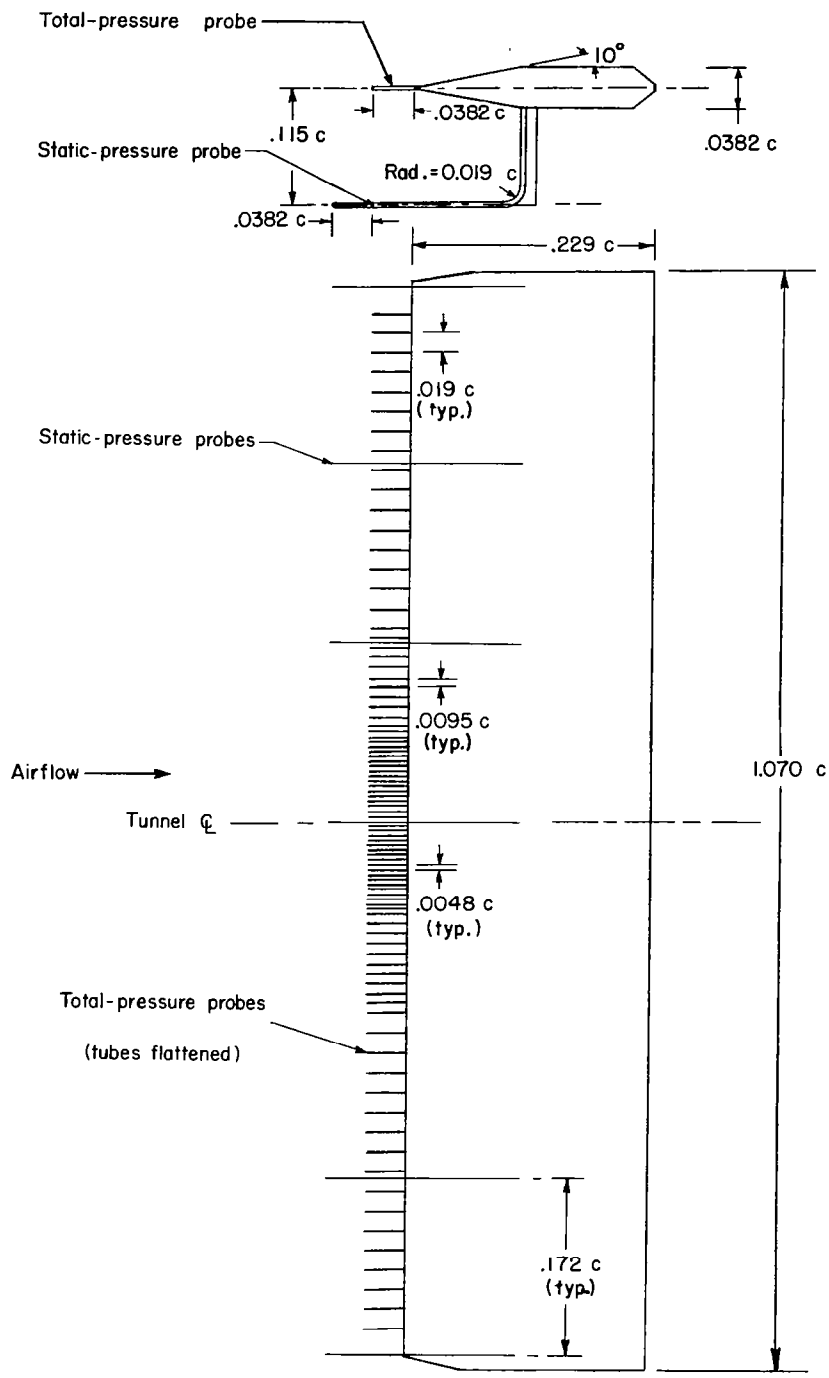

(a) Drawing of wake-survey rake. All dimensions are in terms of model chord, c = 66.47 cm (26.17 in.).

Figure 6.- Wake-survey rake.

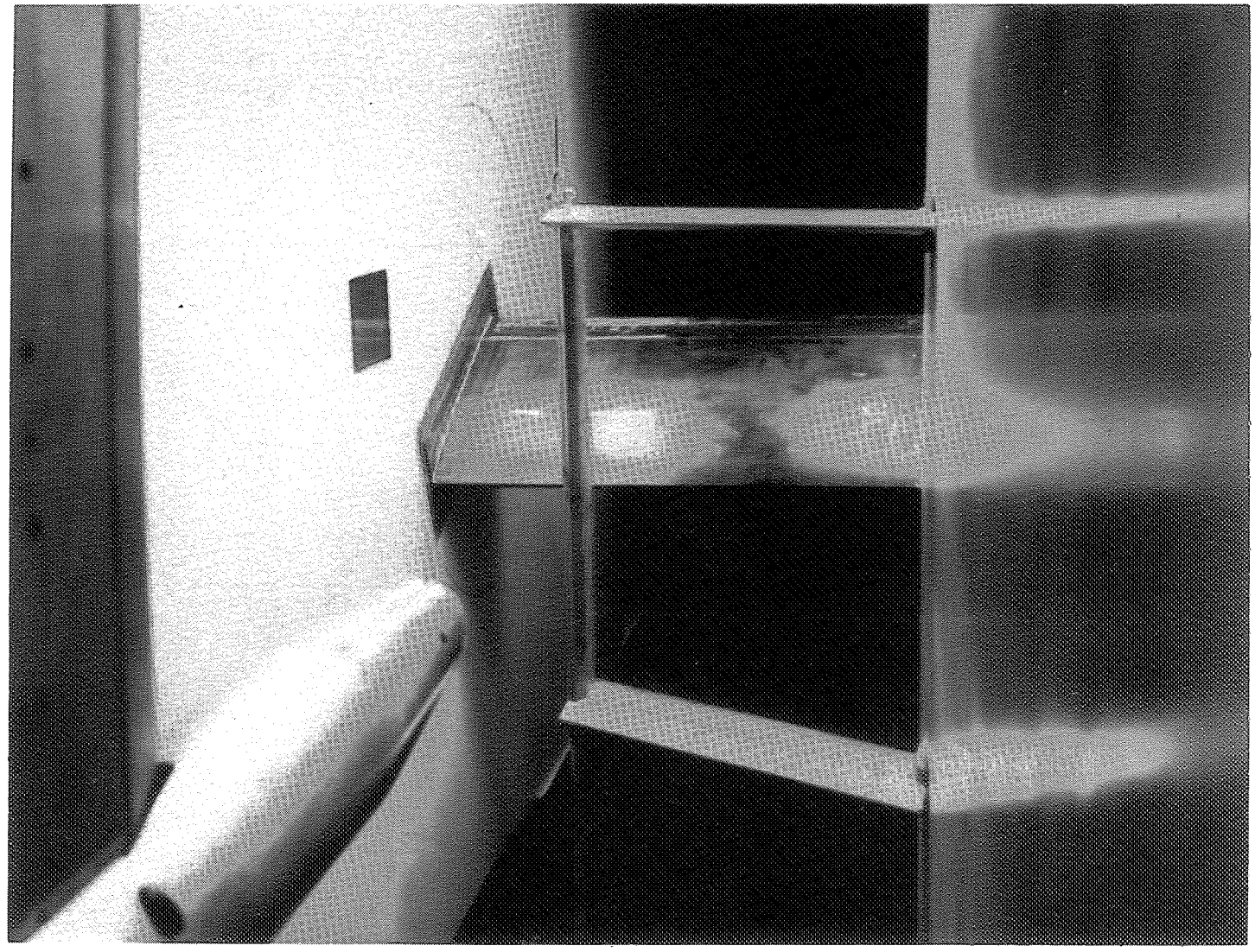

(b) Photograph of wake-survey rake in the Langley low-turbulence pressure tunnel.

Figure 6.- Concluded.

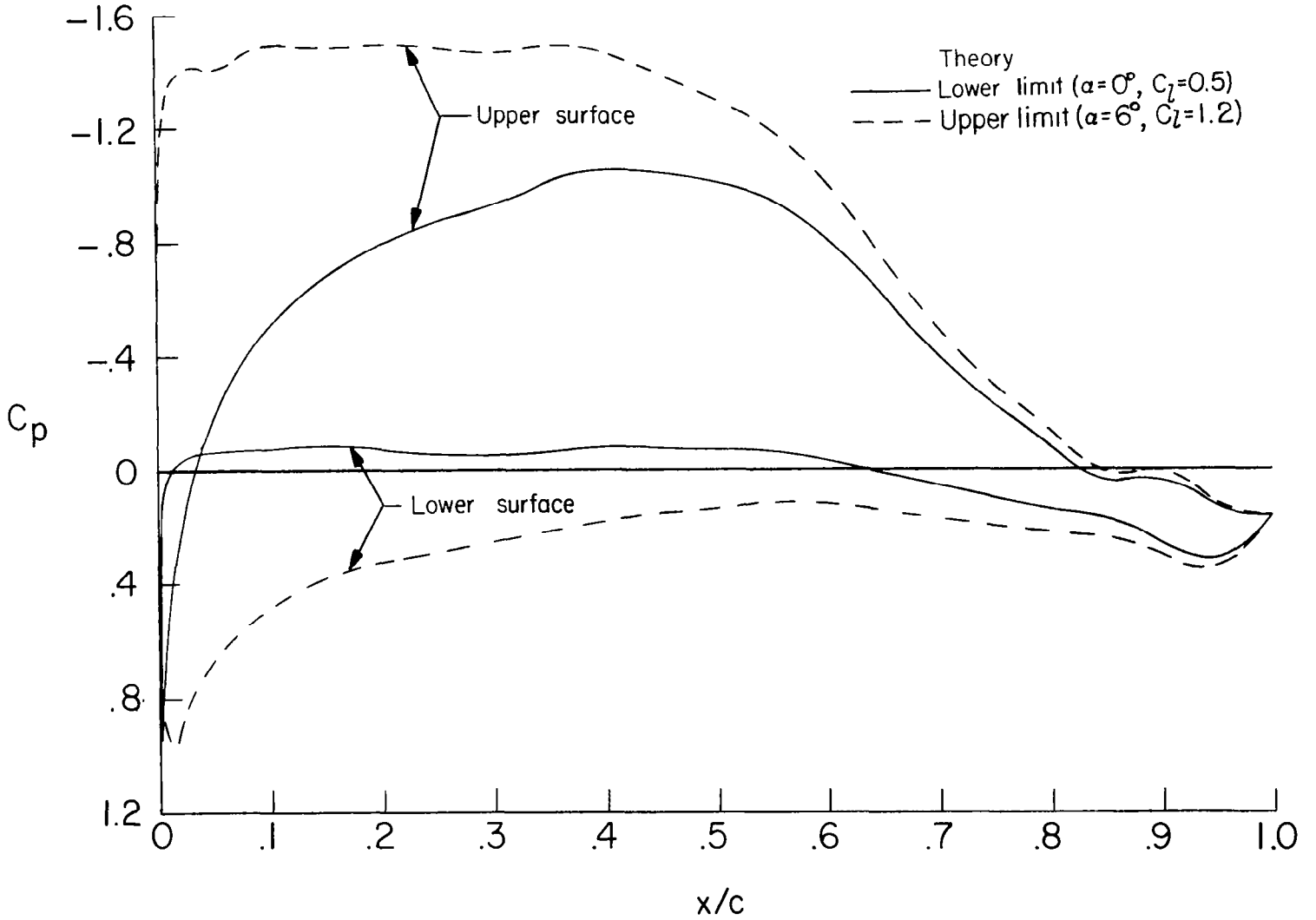

Figure 7.- Theoretical chordwise pressure distributions for configuration 1 (as received) at lower and upper limits of laminar low-drag range for $R = 2.2 \times 10^6$ and $M = 0.10$.

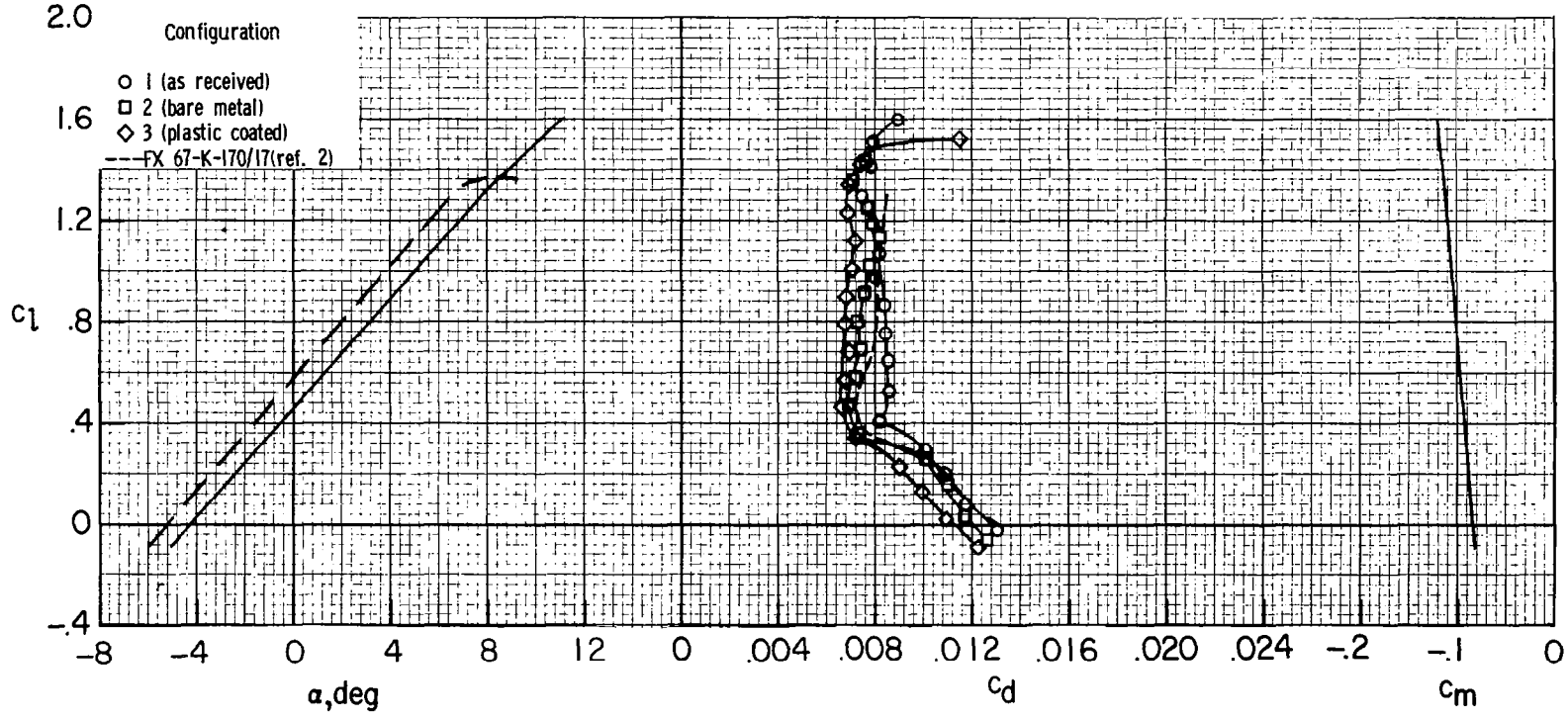

(a) $R = 1.1 \times 10^6$; $M = 0.10$.

Figure 8.- Comparisons of section characteristics of configurations 1 (as received), 2 (bare metal), 3 (plastic-coated), and FX 67-K-170/17 airfoil.

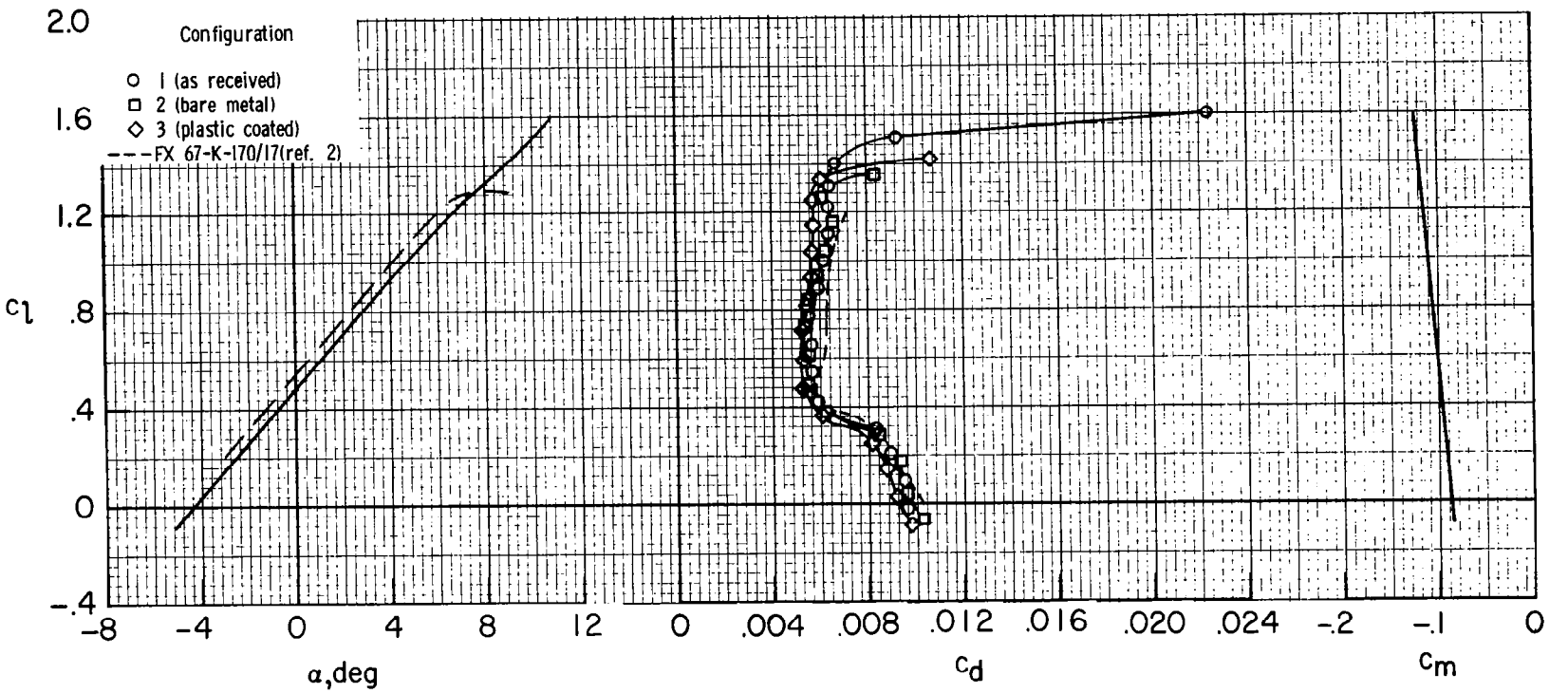

(b) $R = 2.2 \times 10^6$; $M = 0.10$.

Figure 8.- Continued.

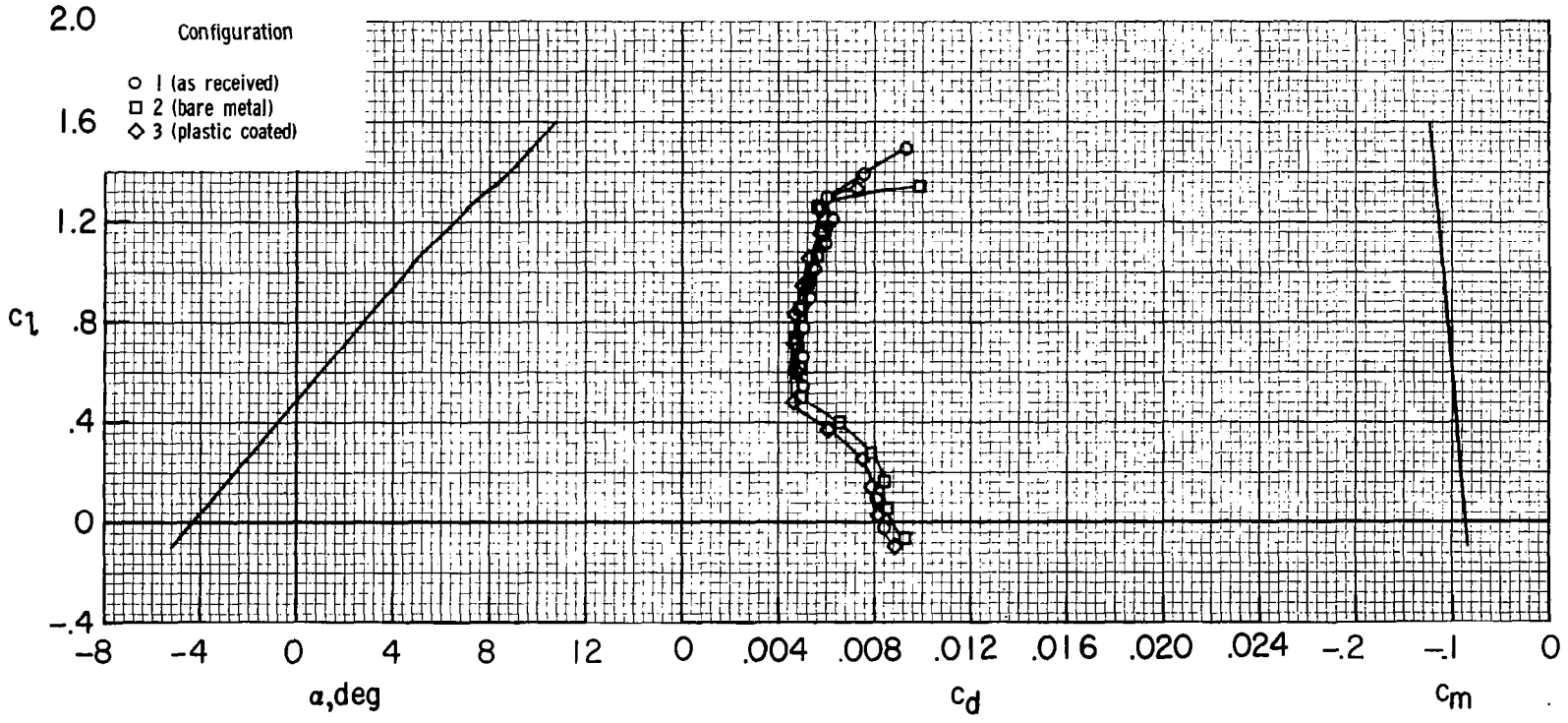

(c) $R = 3.3 \times 10^6$; $M = 0.10$.

Figure 8.- Concluded.

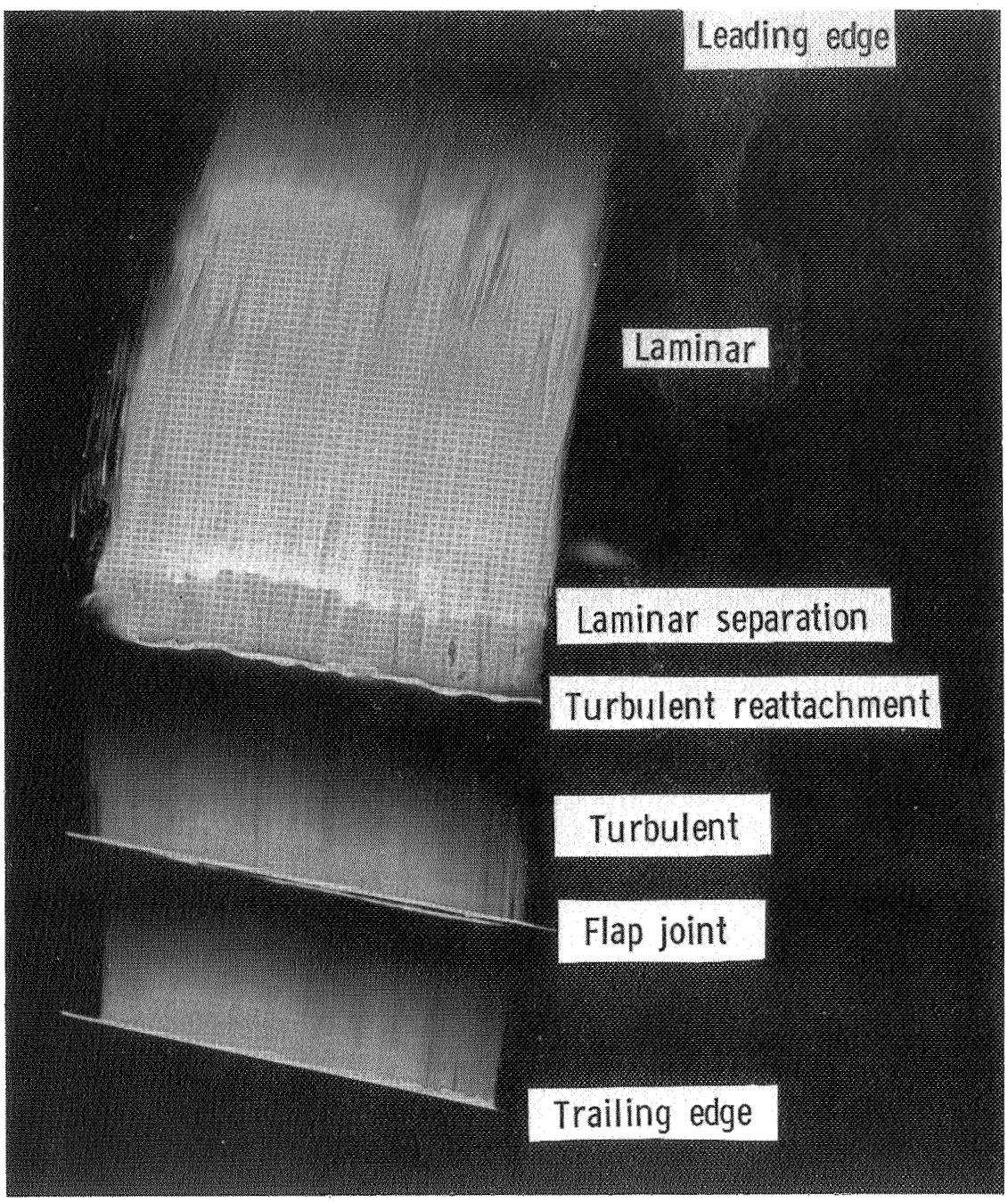

(a) $R \approx 1.1 \times 10^6$, $M = 0.07$, and $\alpha = 0^o$.

Figure 9.- Oil flow photographs of upper surface of configuration 3 (plastic-coated).

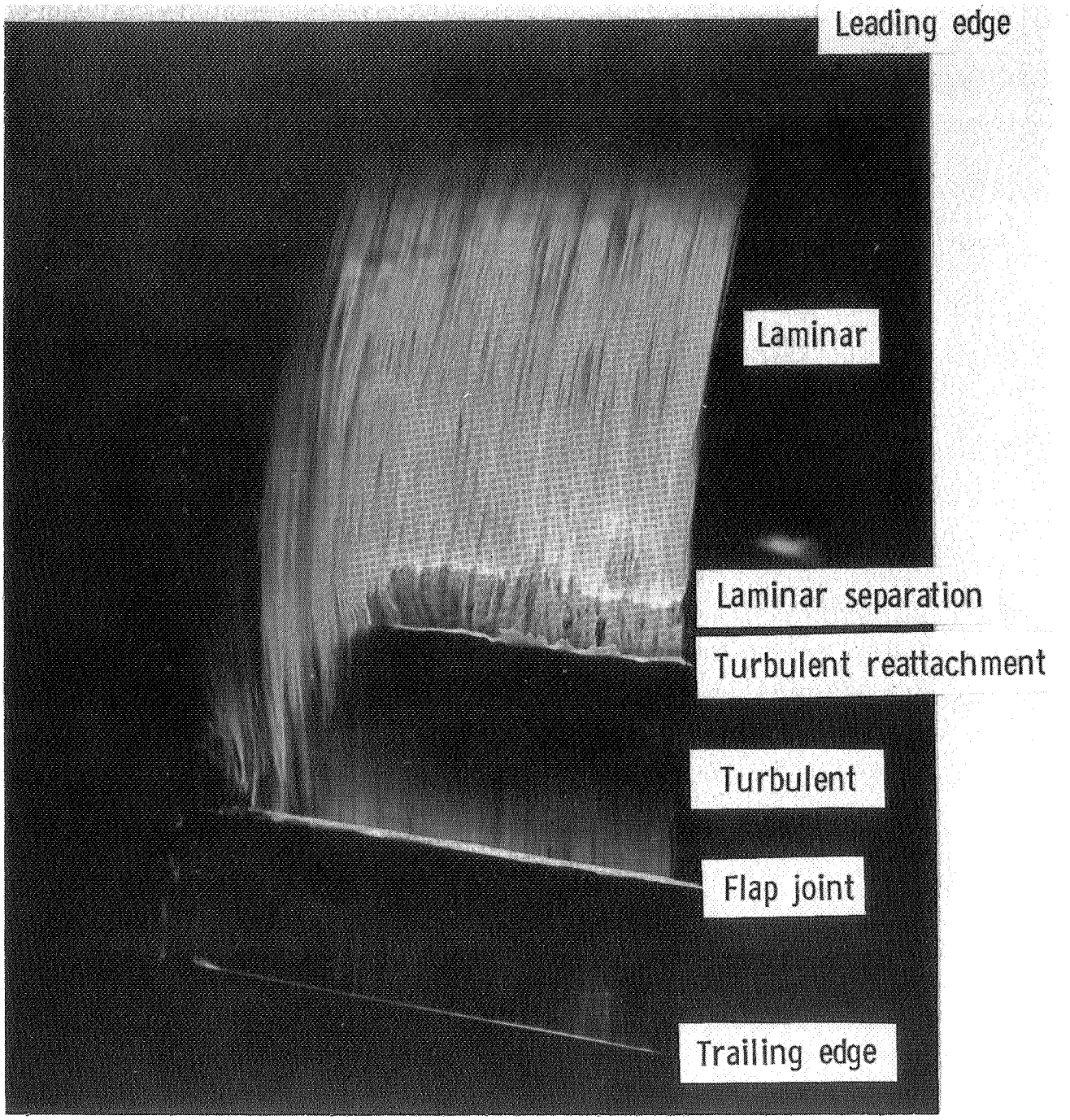

(b) $R \approx 1.5 \times 10^6$, $M = 0.10$, and $\alpha = 0^o$.

Figure 9.- Continued.

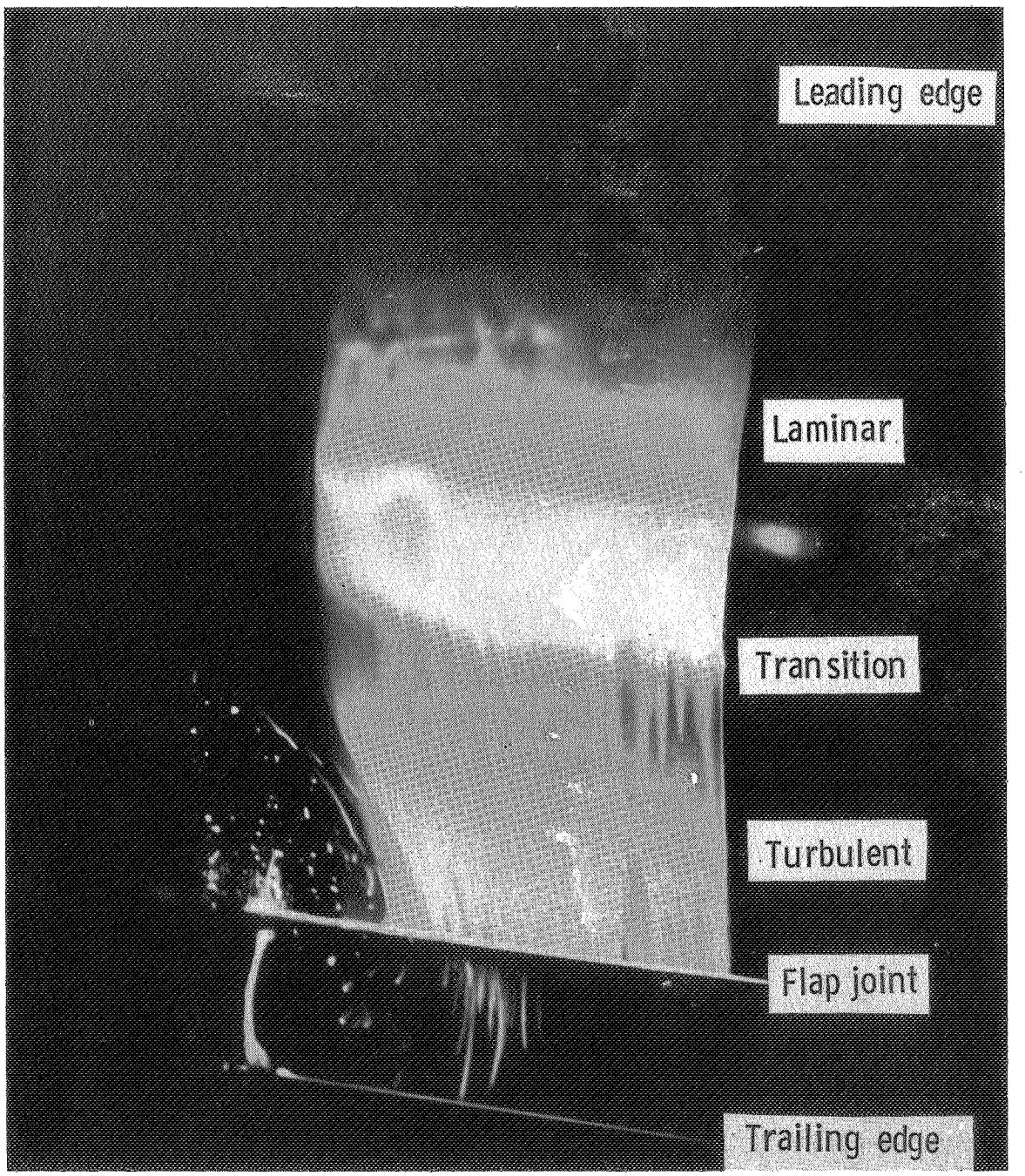

(c) $R \approx 1.5 \times 10^6$, $M = 0.10$, and $\alpha = 7^o$.

Figure 9.- Continued.

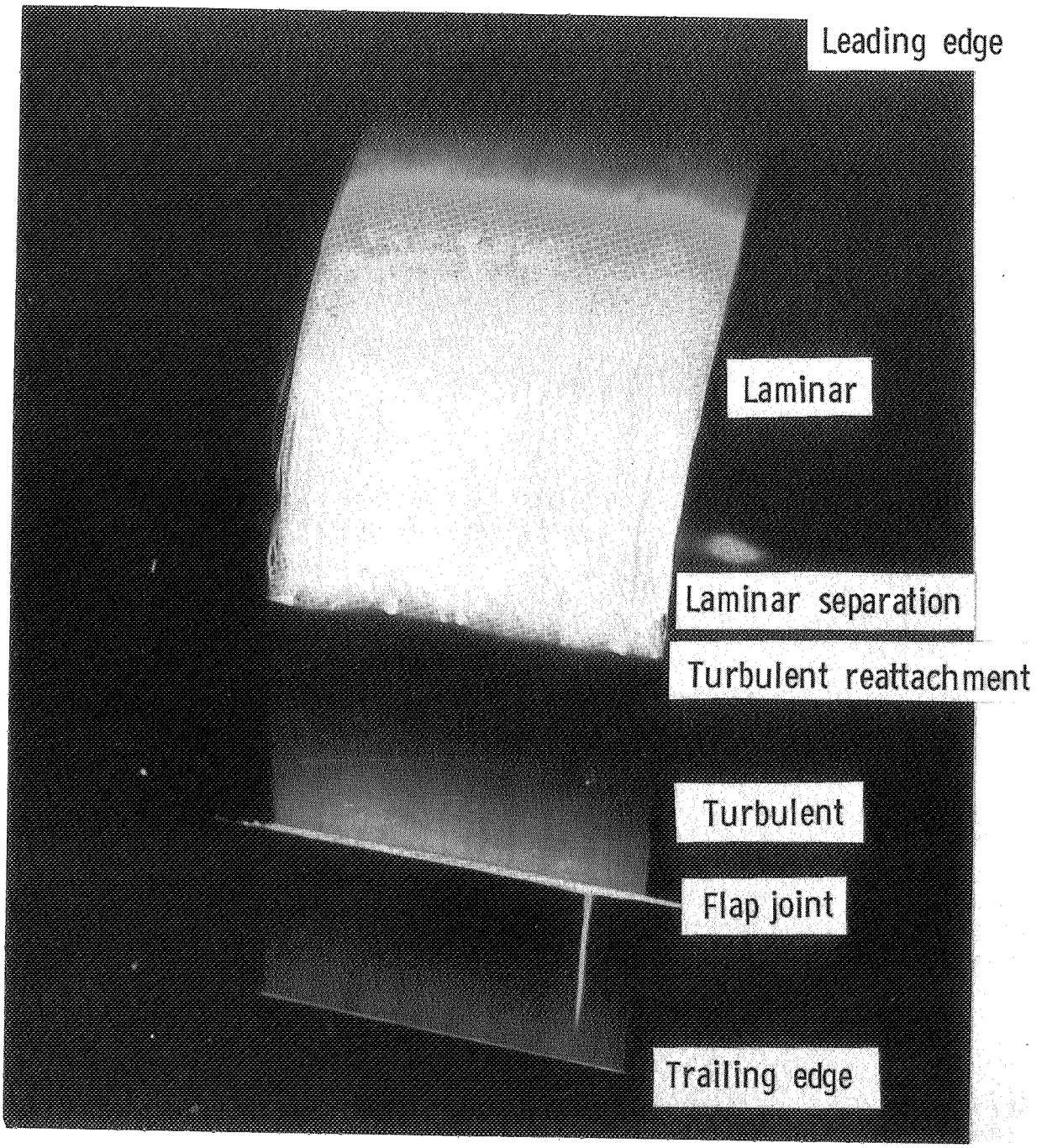

(d) $R \approx 2.5 \times 10^6$, $M = 0.16$, and $\alpha = 0^o$.

Figure 9.- Concluded.